

Cross Sections and Transverse Single-Spin Asymmetries in Forward Neutral Pion Production from Proton Collisions at $\sqrt{s} = 200$ GeV

J. Adams,³ C. Adler,¹² M.M. Aggarwal,²⁵ Z. Ahammed,³⁸ J. Amonett,¹⁷ B.D. Anderson,¹⁷ M. Anderson,⁵ D. Arkhipkin,¹¹ G.S. Averichev,¹⁰ S.K. Badyal,¹⁶ J. Balewski,¹³ O. Barannikova,^{28,10} L.S. Barnby,³ J. Baudot,¹⁵ S. Bekele,²⁴ V.V. Belaga,¹⁰ R. Bellwied,⁴¹ J. Berger,¹² B.I. Bezverkhny,⁴³ S. Bhardwaj,²⁹ P. Bhaskar,³⁸ A.K. Bhati,²⁵ H. Bichsel,⁴⁰ A. Billmeier,⁴¹ L.C. Bland,² C.O. Blyth,³ B.E. Bonner,³⁰ M. Botje,²³ A. Boucham,³⁴ A. Brandin,²¹ A. Bravar,² R.V. Cadman,¹ X.Z. Cai,³³ H. Caines,⁴³ M. Calderón de la Barca Sánchez,² J. Carroll,¹⁸ J. Castillo,¹⁸ M. Castro,⁴¹ D. Cebra,⁵ P. Chaloupka,⁹ S. Chattopadhyay,³⁸ H.F. Chen,³² Y. Chen,⁶ S.P. Chernenko,¹⁰ M. Cherney,⁸ A. Chikanian,⁴³ B. Choi,³⁶ W. Christie,² J.P. Coffin,¹⁵ T.M. Cormier,⁴¹ J.G. Cramer,⁴⁰ H.J. Crawford,⁴ D. Das,³⁸ S. Das,³⁸ A.A. Derevschikov,²⁷ L. Didenko,² T. Dietel,¹² W.J. Dong,⁶ X. Dong,^{32,18} J.E. Draper,⁵ F. Du,⁴³ A.K. Dubey,¹⁴ V.B. Dunin,¹⁰ J.C. Dunlop,² M.R. Dutta Majumdar,³⁸ V. Eckardt,¹⁹ L.G. Efimov,¹⁰ V. Emelianov,²¹ J. Engelage,⁴ G. Eppley,³⁰ B. Erazmus,³⁴ M. Estienne,³⁴ P. Fachini,² V. Faine,² J. Faivre,¹⁵ R. Fatemi,¹³ K. Filimonov,¹⁸ P. Filip,⁹ E. Finch,⁴³ Y. Fisyak,² D. Flierl,¹² K.J. Foley,² J. Fu,⁴² C.A. Gagliardi,³⁵ N. Gagunashvili,¹⁰ J. Gans,⁴³ M.S. Ganti,³⁸ L. Gaudichet,³⁴ M. Germain,¹⁵ F. Geurts,³⁰ V. Ghazikhanian,⁶ P. Ghosh,³⁸ J.E. Gonzalez,⁶ O. Grachov,⁴¹ V. Grigoriev,²¹ S. Gronstal,⁸ D. Grosnick,³⁷ M. Guedon,¹⁵ S.M. Guertin,⁶ A. Gupta,¹⁶ E. Gushin,²¹ T.D. Gutierrez,⁵ T.J. Hallman,² D. Hardtke,¹⁸ J.W. Harris,⁴³ M. Heinz,⁴³ T.W. Henry,³⁵ S. Heppelmann,²⁶ T. Herston,²⁸ B. Hippolyte,⁴³ A. Hirsch,²⁸ E. Hjort,¹⁸ G.W. Hoffmann,³⁶ M. Horsley,⁴³ H.Z. Huang,⁶ S.L. Huang,³² T.J. Humanic,²⁴ G. Igo,⁶ A. Ishihara,³⁶ P. Jacobs,¹⁸ W.W. Jacobs,¹³ M. Janik,³⁹ H. Jiang,^{6,18} I. Johnson,¹⁸ P.G. Jones,³ E.G. Judd,⁴ S. Kabana,⁴³ M. Kaneta,¹⁸ M. Kaplan,⁷ D. Keane,¹⁷ V.Yu. Khodyrev,²⁷ J. Kiryluk,⁶ A. Kisiel,³⁹ J. Klay,¹⁸ S.R. Klein,¹⁸ A. Klyachko,¹³ D.D. Koetke,³⁷ T. Kollegger,¹² M. Kopytine,¹⁷ L. Kotchenda,²¹ A.D. Kovalenko,¹⁰ M. Kramer,²² P. Kravtsov,²¹ V.I. Kravtsov,²⁷ K. Krueger,¹ C. Kuhn,¹⁵ A.I. Kulikov,¹⁰ A. Kumar,²⁵ G.J. Kunde,⁴³ C.L. Kunz,⁷ R.Kh. Kutuev,¹¹ A.A. Kuznetsov,¹⁰ M.A.C. Lamont,³ J.M. Landgraf,² S. Lange,¹² C.P. Lansdell,³⁶ B. Lasiuk,⁴³ F. Laue,² J. Lauret,² A. Lebedev,² R. Lednický,¹⁰ M.J. LeVine,² C. Li,³² Q. Li,⁴¹ S.J. Lindenbaum,²² M.A. Lisa,²⁴ F. Liu,⁴² L. Liu,⁴² Z. Liu,⁴² Q.J. Liu,⁴⁰ T. Ljubicic,² W.J. Llope,³⁰ H. Long,⁶ R.S. Longacre,² M. Lopez-Noriega,²⁴ W.A. Love,² T. Ludlam,² D. Lynn,² J. Ma,⁶ Y.G. Ma,³³ D. Magestro,²⁴ S. Mahajan,¹⁶ L.K. Mangotra,¹⁶ D.P. Mahapatra,¹⁴ R. Majka,⁴³ R. Manweiler,³⁷ S. Margetis,¹⁷ C. Markert,⁴³ L. Martin,³⁴ J. Marx,¹⁸ H.S. Matis,¹⁸ Yu.A. Matulenko,²⁷ T.S. McShane,⁸ F. Meissner,¹⁸ Yu. Melnick,²⁷ A. Meschanin,²⁷ M. Messer,² M.L. Miller,⁴³ Z. Milosevich,⁷ N.G. Minaev,²⁷ C. Mironov,¹⁷ D. Mishra,¹⁴ J. Mitchell,³⁰ B. Mohanty,³⁸ L. Molnar,²⁸ C.F. Moore,³⁶ M.J. Mora-Corral,¹⁹ D.A. Morozov,²⁷ V. Morozov,¹⁸ M.M. de Moura,³¹ M.G. Munhoz,³¹ B.K. Nandi,³⁸ S.K. Nayak,¹⁶ T.K. Nayak,³⁸ J.M. Nelson,³ P. Nevski,² V.A. Nikitin,¹¹ L.V. Nogach,²⁷ B. Norman,¹⁷ S.B. Nurushev,²⁷ G. Odyniec,¹⁸ A. Ogawa,² V. Okorokov,²¹ M. Oldenburg,¹⁸ D. Olson,¹⁸ G. Paic,²⁴ S.U. Pandey,⁴¹ S.K. Pal,³⁸ Y. Panebratsev,¹⁰ S.Y. Panitkin,² A.I. Pavlinov,⁴¹ T. Pawlak,³⁹ V. Perevoztchikov,² C. Perkins,⁴ W. Peryt,³⁹ V.A. Petrov,¹¹ S.C. Phatak,¹⁴ R. Picha,⁵ M. Planinic,⁴⁴ J. Pluta,³⁹ N. Porile,²⁸ J. Porter,² A.M. Poskanzer,¹⁸ M. Potekhin,² E. Potrebenikova,¹⁰ B.V.K.S. Potukuchi,¹⁶ D. Prindle,⁴⁰ C. Pruneau,⁴¹ J. Putschke,¹⁹ G. Rai,¹⁸ G. Rakness,¹³ R. Raniwala,²⁹ S. Raniwala,²⁹ O. Ravel,³⁴ R.L. Ray,³⁶ S.V. Razin,^{10,13} D. Reichhold,²⁸ J.G. Reid,⁴⁰ G. Renault,³⁴ F. Retiere,¹⁸ A. Ridiger,²¹ H.G. Ritter,¹⁸ J.B. Roberts,³⁰ O.V. Rogachevski,¹⁰ J.L. Romero,⁵ A. Rose,⁴¹ C. Roy,³⁴ L.J. Ruan,^{32,2} R. Sahoo,¹⁴ I. Sakrejda,¹⁸ S. Salur,⁴³ J. Sandweiss,⁴³ I. Savin,¹¹ J. Schambach,³⁶ R.P. Scharenberg,²⁸ N. Schmitz,¹⁹ L.S. Schroeder,¹⁸ K. Schweda,¹⁸ J. Seger,⁸ D. Seliverstov,²¹ P. Seyboth,¹⁹ E. Shabaliev,¹⁰ M. Shao,³² M. Sharma,²⁵ K.E. Shestermanov,²⁷ S.S. Shimanskii,¹⁰ R.N. Singaraju,³⁸ F. Simon,¹⁹ G. Skoro,¹⁰ N. Smirnov,⁴³ R. Snellings,²³ G. Sood,²⁵ P. Sorensen,¹⁸ J. Sowinski,¹³ H.M. Spinka,¹ B. Srivastava,²⁸ S. Stanislaus,³⁷ R. Stock,¹² A. Stolpovsky,⁴¹ M. Strikhanov,²¹ B. Stringfellow,²⁸ C. Struck,¹² A.A.P. Suaide,³¹ E. Sugarbaker,²⁴ C. Suire,² M. Šumbera,⁹ B. Surov,² T.J.M. Symons,¹⁸ A. Szanto de Toledo,³¹ P. Szarwas,³⁹ A. Tai,⁶ J. Takahashi,³¹ A.H. Tang,^{2,23} D. Thein,⁶ J.H. Thomas,¹⁸ V. Tikhomirov,²¹ M. Tokarev,¹⁰ M.B. Tonjes,²⁰ T.A. Trainor,⁴⁰ S. Trentalange,⁶ R.E. Tribble,³⁵ M.D. Trivedi,³⁸ V. Trofimov,²¹ O. Tsai,⁶ T. Ullrich,² D.G. Underwood,¹ G. Van Buren,² A.M. VanderMolen,²⁰ A.N. Vasiliev,²⁷ M. Vasiliev,³⁵ S.E. Vigdor,¹³ Y.P. Viyogi,³⁸ S.A. Voloshin,⁴¹ W. Wagoner,⁸ F. Wang,²⁸ G. Wang,¹⁷ X.L. Wang,³² Z.M. Wang,³² H. Ward,³⁶ J.W. Watson,¹⁷ R. Wells,²⁴ G.D. Westfall,²⁰ C. Whitten Jr.,⁶ H. Wieman,¹⁸ R. Willson,²⁴ S.W. Wissink,¹³ R. Witt,⁴³ J. Wood,⁶ J. Wu,³² N. Xu,¹⁸ Z. Xu,² Z.Z. Xu,³² E. Yamamoto,¹⁸ P. Yepes,³⁰ V.I. Yurevich,¹⁰ Y.V. Zanevski,¹⁰ I. Zborovský,⁹ H. Zhang,^{43,2}

W.M. Zhang,¹⁷ Z.P. Zhang,³² P.A. Żolnierczuk,¹³ R. Zoukarneev,¹¹ J. Zoukarneeva,¹¹ and A.N. Zubarev¹⁰

(STAR Collaboration),*

- ¹Argonne National Laboratory, Argonne, Illinois 60439
²Brookhaven National Laboratory, Upton, New York 11973
³University of Birmingham, Birmingham, United Kingdom
⁴University of California, Berkeley, California 94720
⁵University of California, Davis, California 95616
⁶University of California, Los Angeles, California 90095
⁷Carnegie Mellon University, Pittsburgh, Pennsylvania 15213
⁸Creighton University, Omaha, Nebraska 68178
⁹Nuclear Physics Institute AS CR, Řež/Prague, Czech Republic
¹⁰Laboratory for High Energy (JINR), Dubna, Russia
¹¹Particle Physics Laboratory (JINR), Dubna, Russia
¹²University of Frankfurt, Frankfurt, Germany
¹³Indiana University, Bloomington, Indiana 47408
¹⁴Institute of Physics, Bhubaneswar 751005, India
¹⁵Institut de Recherches Subatomiques, Strasbourg, France
¹⁶University of Jammu, Jammu 180001, India
¹⁷Kent State University, Kent, Ohio 44242
¹⁸Lawrence Berkeley National Laboratory, Berkeley, California 94720
¹⁹Max-Planck-Institut für Physik, Munich, Germany
²⁰Michigan State University, East Lansing, Michigan 48824
²¹Moscow Engineering Physics Institute, Moscow Russia
²²City College of New York, New York City, New York 10031
²³NIKHEF, Amsterdam, The Netherlands
²⁴Ohio State University, Columbus, Ohio 43210
²⁵Panjab University, Chandigarh 160014, India
²⁶Pennsylvania State University, University Park, Pennsylvania 16802
²⁷Institute of High Energy Physics, Protvino, Russia
²⁸Purdue University, West Lafayette, Indiana 47907
²⁹University of Rajasthan, Jaipur 302004, India
³⁰Rice University, Houston, Texas 77251
³¹Universidade de Sao Paulo, Sao Paulo, Brazil
³²University of Science & Technology of China, Anhui 230027, China
³³Shanghai Institute of Nuclear Research, Shanghai 201800, P.R. China
³⁴SUBATECH, Nantes, France
³⁵Texas A&M, College Station, Texas 77843
³⁶University of Texas, Austin, Texas 78712
³⁷Valparaiso University, Valparaiso, Indiana 46383
³⁸Variable Energy Cyclotron Centre, Kolkata 700064, India
³⁹Warsaw University of Technology, Warsaw, Poland
⁴⁰University of Washington, Seattle, Washington 98195
⁴¹Wayne State University, Detroit, Michigan 48201
⁴²Institute of Particle Physics, CCNU (HZNU), Wuhan, 430079 China
⁴³Yale University, New Haven, Connecticut 06520
⁴⁴University of Zagreb, Zagreb, HR-10002, Croatia

(Dated: October 30, 2003)

Measurements of the production of high energy π^0 mesons at large pseudorapidity and $15 < E_\pi < 80$ GeV from the collisions of transversely polarized protons at $\sqrt{s} = 200$ GeV are reported. The invariant differential cross section is generally consistent with next-to-leading order perturbative QCD calculations. The analyzing power is found to be large and positive, similar to that observed in fixed-target data at $\sqrt{s} \leq 20$ GeV, increasing from zero with Feynman- x (x_F) for $x_F \gtrsim 0.3$. The analyzing power is in qualitative agreement with perturbative QCD model expectations extrapolated from the lower energy data. This is the first significant spin result seen for particles produced with transverse momentum above 1 GeV/c at a polarized proton collider.

PACS numbers: 13.85.Ni, 13.88+e, 12.38.Qk

An early qualitative expectation from perturbative Quantum Chromodynamics (pQCD) was that the chiral properties of the theory would make transverse single-

spin asymmetries for inclusive particle production be very small [1]. Contrary to this expectation, measurements of the analyzing power (A_N) for the production

of pions in $p_{\uparrow} + p$ collisions at center-of-mass energies $\sqrt{s} \leq 20$ GeV and moderate transverse momentum ($0.5 \leq p_T \leq 2.0$ GeV/c) were found to be large. For neutral and charged pion production at large Feynman- x ($x_F = 2p_L/\sqrt{s}$, where p_L is the longitudinal momentum of the pion), A_N was measured to be 20–40% [2, 3, 4, 5]. Recently, fixed-target semi-inclusive lepton scattering experiments have also reported measurements of transverse single-spin asymmetries which are significantly different from zero [6, 7]. These results have sparked substantial theoretical activity to gain an understanding of these transverse spin effects within the framework of pQCD [8].

Perturbative QCD calculations of pion production involve the convolution of parton distribution and fragmentation functions with a hard partonic interaction. The reliability of calculations in the pQCD framework is expected to increase as p_T gets larger. In this framework, forward π production in $p + p$ collisions is dominated by scattering of a valence quark in one proton from a low Bjorken- x gluon in the other. At large pseudorapidities (η) and $\sqrt{s} \leq 20$ GeV, there may be significant contributions to particle production from soft hadronic processes collectively known as beam fragmentation. At a collider, \sqrt{s} is significantly larger, leading to the expectation that the origin of forward pions will shift towards collisions involving the partonic constituents of the proton, consistent with PYTHIA simulations [9]. Measurements of the cross section for forward pion production are important to establish that pQCD is a suitable framework for treating polarization observables in these kinematics.

Different mechanisms have been identified in the pQCD framework by which one might expect transverse spin effects [10, 11, 12, 13, 14, 15], all of which may contribute to some degree. With only data at $\sqrt{s} \leq 20$ GeV for comparison, these models are not well constrained. Despite this, the models have been extrapolated by an order of magnitude in \sqrt{s} and approximately a factor of 2 in p_T , and all predict that sizable transverse spin effects will persist at $\sqrt{s} = 200$ GeV. This Letter addresses the question if A_N is sizable at $\sqrt{s} = 200$ GeV, as predicted by these models. We present measurements of the cross section and A_N for the production of forward π^0 mesons having $p_T > 1$ GeV/c from $p_{\uparrow} + p$ collisions at $\sqrt{s} = 200$ GeV.

Data were collected by the STAR experiment (Solenoid Tracker at RHIC) at the Relativistic Heavy Ion Collider (RHIC) in January 2002. RHIC is the first polarized proton collider. Polarization is produced by optical pumping of an atomic-beam source [16] and is partially preserved through an accelerator complex to reach RHIC [17]. In RHIC, a pair of helical dipole magnets in each ring serve as the first application of full “Siberian snakes” [18] in a high-energy accelerator to preserve polarization through numerous depolarizing resonances during acceleration of the beam. The stable spin axis of the RHIC rings is vertical. Proton beam bunches crossed the STAR interaction

region (IR) every 213 nsec. The polarization direction alternated between up and down for successive bunches of one beam, and for every second bunch of the other beam. Data were sorted according to the polarization direction of the beam corresponding to positive x_F particle production. Averaging over the polarization in the other beam resulted in negligible remnant polarization. Typical collision luminosities were about 10^{30} cm⁻²sec⁻¹. The integrated luminosity was about 150 nb⁻¹ for these measurements.

The average beam polarization for each fill, P_{beam} , was measured by a Coulomb-Nuclear Interference (CNI) polarimeter located in RHIC [19, 20]. At 24.3 GeV, the RHIC injection energy, the analyzing power of the CNI reaction is $A_N^{CNI} = 0.0133 \pm 0.0041$ [21, 22], and can be used to deduce the absolute polarization of the proton beam. However, at 100 GeV, the beam energy used for RHIC collisions, A_N^{CNI} has not yet been measured. The CNI asymmetries measured at injection and collision energies were nearly equal for many fills. Since the beam acceleration process is unlikely to increase P_{beam} , this suggests that A_N^{CNI} at 100 GeV is no smaller than at 24.3 GeV. For the present analysis, we assume there is no change in A_N^{CNI} between these two energies, giving an average value of $\langle P_{beam} \rangle = 0.16$ for the data presented here.

A prototype forward π^0 detector (pFPD) was installed at STAR near the beam pipe 750 cm from the IR. The pFPD consisted of an electromagnetic Pb-scintillator sampling calorimeter [23], placed with its edge ≈ 30 cm left of the oncoming polarized proton beam. The pFPD was 21 radiation lengths deep and subdivided into 4×3 towers. To measure the transverse profiles of photon showers, the pFPD had a shower-maximum detector (SMD) located near the most-probable depth for maximum energy deposition from the showers. The SMD comprised two orthogonal layers of 100×60 scintillator strips spaced at 0.37 cm. To address systematic uncertainties associated with measuring left-right asymmetries with a single arm detector, 4×4 arrays of Pb-glass detectors with no SMD were placed to the right of, above, and below the oncoming polarized proton beam.

The luminosity was measured at STAR using beam-beam counters (BBC) [24] composed of segmented scintillator annuli mounted around the beam at longitudinal positions $z = \pm 370$ cm, spanning $3.3 < |\eta| < 5.0$. Proton collision events were identified by requiring the coincidence of at least one BBC segment fore and aft of the IR. Absolute luminosity was determined by measuring the transverse size of the colliding beams and the number of protons colliding at STAR. The cross section measured with the BBC is $26.1 \pm 0.2(\text{stat.}) \pm 1.8(\text{syst.})$ mb [25], consistent with simulation [9, 26]. The BBC observes $87 \pm 8\%$ of the inelastic, non-singly diffractive cross section.

All forward calorimeters were read out for events that deposited $\gtrsim 15$ GeV electron-equivalent energy in any

one calorimeter. The BBC coincidence requirement was imposed to select events from proton-proton collisions.

A measurement of A_N with a single arm detector to the left, such as the pFPD, is given by the expression

$$P_{beam}A_N = \frac{N_+ - RN_-}{N_+ + RN_-}. \quad (1)$$

The number of π^0 mesons detected when the beam spin vector was oriented up (down) is $N_{+(-)}$. The spin-dependent relative luminosity ($R = \mathcal{L}_+/\mathcal{L}_- \approx 1.15$) was measured with the BBC. Background contributions to the relative luminosity determination were reduced by increasing the coincidence requirements to at least two BBC segments on each side of STAR. The systematic uncertainties for the spin-dependent relative luminosities measured with the BBC are on the order of 10^{-3} [24], a factor of 10 to 20 smaller than $P_{beam}A_N$ measured with the pFPD.

Neutral π mesons are reconstructed using events with at least two clusters in the SMD according to the formula

$$M_{\gamma\gamma} = E_\pi \sqrt{1 - z_\gamma^2} \sin\left(\frac{\phi_{\gamma\gamma}}{2}\right) \approx E_{tot} \sqrt{1 - z_\gamma^2} \frac{d_{\gamma\gamma}}{2z_{vtx}}. \quad (2)$$

The energy of the leading π^0 , E_π , is taken to be the total energy deposited in all of the towers, E_{tot} , assumed to be electromagnetic. The opening angle between the photons, $\phi_{\gamma\gamma}$, is determined by z_{vtx} , the longitudinal distance between the collision vertex and the detector, and the distance between the two photons at the calorimeter, $d_{\gamma\gamma}$. Both $d_{\gamma\gamma}$ and the energy sharing parameter, $z_\gamma = |E_{\gamma 1} - E_{\gamma 2}|/(E_{\gamma 1} + E_{\gamma 2})$, are measured by an analysis of the energy deposited in the strips of the SMD planes. The value of $d_{\gamma\gamma}$ is determined from the fitted centroids of the two peaks, while z_γ is determined from the fitted area under each peak. A fiducial volume is defined by requiring the SMD peaks to be more than 12 strips from the detector edge. Figure 1 shows the $M_{\gamma\gamma}$ spectra for two energy bins. The mass resolution is 20 MeV/c² (RMS) for π^0 energies from 15–80 GeV, limited by the measurement of $\phi_{\gamma\gamma}$. The centroid of the π^0 peak is used to determine the absolute energy scale for each tower for each fill to an accuracy of order 1%. The energy scale is found to have negligible dependence on energy or spin-state.

The π^0 detection efficiency is determined in a matrix of E_π and η from a simulation using PYTHIA [9] to model the $p_\uparrow + p$ collisions and GEANT [26] to model the detector response. The open histograms in Fig. 1 are simulation events which undergo the same reconstruction and selection as the data. The simulation matches the data well for several kinematic variables, including p_T , E_{tot} , and η . The π^0 detection efficiency is dominated by the geometrical acceptance of the calorimeter.

The π^0 sample is distorted by coincident particles from the jet containing the π^0 . The pFPD is about one

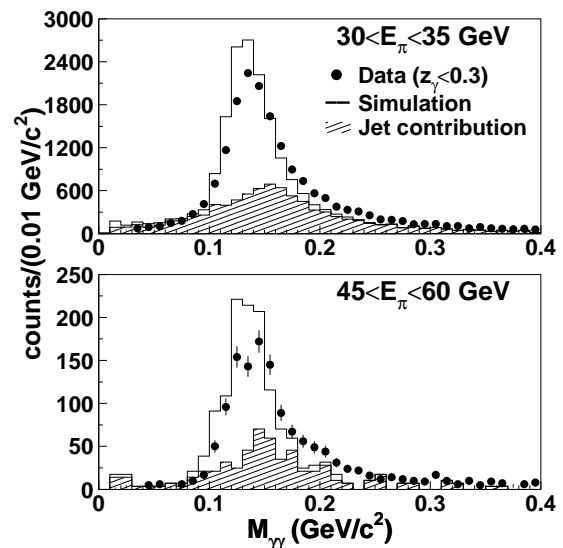


FIG. 1: Uncorrected spectra of the diphoton invariant mass in two energy bins. The points are data. The open histograms are reconstructed simulation events, normalized to equal area as the data. The hatched histograms are simulation events used to correct the cross section, described in the text. The error bars on the data represent the statistical uncertainty.

hadronic interaction length deep. When events with two photons from π^0 decays overlap with other particles, the detection of the other particles tends to increase E_{tot} relative to E_π and broadens the $\phi_{\gamma\gamma}$ resolution. This results in a broad invariant mass distribution peaked at a value larger than M_π . The average value of E_{tot} is approximately 3 GeV larger than E_π , independent of E_π . Simulation events with $|E_{tot} - E_\pi| > 2$ GeV are shown as the hatched histograms in Fig. 1. Events with only one photon from π^0 decay plus other particles exist predominantly at small $M_{\gamma\gamma}$, and are suppressed by imposing the constraint $z_\gamma < 0.3$. The E_π -dependent systematic uncertainty in the cross section is about 20%, dominated by the jet contribution correction. The simulation used for the efficiency correction includes π^0 events together with the jet contribution. The uncertainty includes the difference when these effects are explicitly corrected in both the data and the simulation, and when they are corrected in neither.

Non-collision background is suppressed to the level of 1% by requiring the coincidence from the BBC in the offline analysis. Following our simulations, the cross section is corrected by 10% to account for the bias introduced by the BBC coincidence condition. Hadronic background comprising events with no leading π^0 in the acceptance of the calorimeter is predominantly at small $M_{\gamma\gamma}$, and is reduced by constraining z_γ . The hadronic background amounts to about 2% of the yield underneath the π^0 peak at $0.09 < M_{\gamma\gamma} < 0.22$ GeV/c².

The differential cross section for inclusive π^0 production for $30 < E_\pi < 55$ GeV in 5 GeV bins is presented

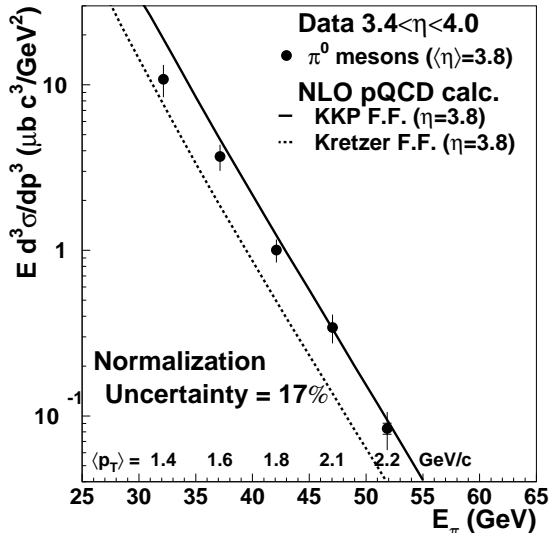


FIG. 2: Invariant differential cross section for inclusive π^0 production versus leading π^0 energy. The inner error bars are the statistical uncertainty, and are smaller than the symbols for most data points. The outer error bars are the statistical and E_π -dependent systematic uncertainties added in quadrature. The curves are NLO pQCD calculations evaluated at $\eta = 3.8$ using different fragmentation functions [27, 30, 31].

in Fig. 2. Data with $3.4 < \eta < 4.0$ were selected, giving $\langle \eta \rangle = 3.8$ independent of E_π ; in this range the detector efficiency is well understood. The dominant contributions to the normalization uncertainty come from knowledge of the absolute transverse position of the detector (10%), the absolute luminosity determination (8%), and the model dependence of the BBC efficiency (8%). The data are plotted at the average E_π of the bin.

The curves on the plot are next-to-leading order (NLO) pQCD calculations [27] evaluated at $\eta = 3.8$, using the CTEQ6M [28] parton distribution functions and equal renormalization and factorization scales of p_T . The NLO pQCD calculations are in general consistent with the data, in contrast to midrapidity π^0 data at lower \sqrt{s} [29]. The solid line uses the “Kniehl-Kramer-Pötter” (KKP) set of fragmentation functions [30], while the dashed line uses the “Kretzer” set [31]. The difference between the two reflects uncertainties in the fragmentation functions at these kinematics. At the chosen scale, the KKP fragmentation functions tend to agree with the data better than Kretzer, consistent with what has been observed for midrapidity π^0 data at $\sqrt{s} = 200$ GeV [32].

The analyzing power is presented in Fig. 3, plotted versus $2 \langle E_{tot} \rangle / \sqrt{s} \approx x_F$. The average p_T is correlated with x_F , as the pFPD was at a fixed angle relative to the collision point. The solid points are π^0 mesons from $3.3 < \eta < 4.1$ and $0.07 < M_{\gamma\gamma} < 0.3$ GeV/ c^2 , with x_F -dependent constraints on z_γ to minimize hadronic background. The open points are based solely on the total electromagnetic energy in the pFPD without SMD

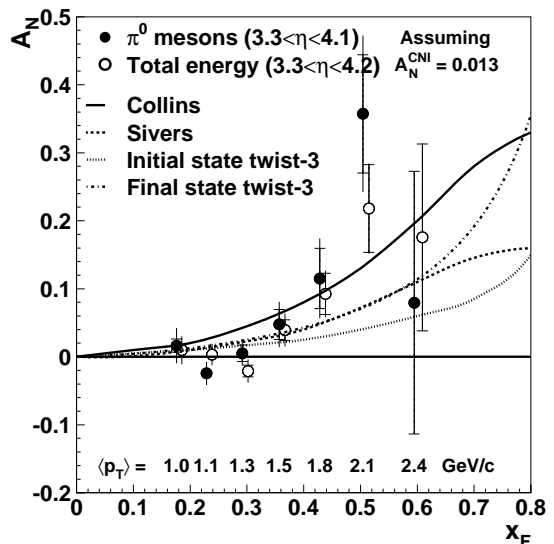


FIG. 3: Analyzing powers versus x_F . The solid points are identified π^0 mesons. The open points are the total energy deposited in the calorimeter, shifted by $x_F = +0.01$ to ease viewing. The inner error bars are the statistical uncertainty, and the outer error bars are the statistical and point-to-point systematic uncertainties added in quadrature. The curves are predictions from pQCD models evaluated at $p_T = 1.5$ GeV/ c [12, 13, 14, 15]. The measured A_N values are proportional to A_N^{CNI} at 100 GeV, which is assumed to be 0.013 as described in the text.

analysis: neither fiducial volume constraints nor π^0 identification. The agreement between the solid and open points indicates A_N is not sensitive to the analysis used to identify π^0 mesons. This is consistent with simulations showing that 95% of events with at least 25 GeV deposited in the pFPD come from photons, 95% of which are daughters from π^0 decay. The A_N seen at beam-right with the Pb-glass array is similar to that seen at beam-left with the pFPD, while A_N for the Pb-glass above and below the beam is consistent with zero, as expected. The largest x_F -dependent systematic uncertainty for A_N arises from comparison of the beam-left and beam-right data. The average $A_N(x_F)$ is computed using the beam-left and beam-right data, and a systematic uncertainty is assigned to bring the beam-left $A_N(x_F)$ (shown in Fig. 3) within one standard deviation of the average.

The curves on the plot are predictions from the pQCD models, fitted to data at $\sqrt{s} = 20$ GeV, extrapolated to $\sqrt{s} = 200$ GeV and evaluated at $p_T = 1.5$ GeV/ c [12, 13, 14, 15]. One model attributes single-spin effects to the convolution of the transversity distribution function with a spin-dependent Collins fragmentation function [12]. The Sivers model adds explicit spin-dependent k_T dependence to the parton distribution functions [13]. Other models ascribe the effects to twist-3 parton correlations in the initial or final state [14, 15]. The data are qualitatively consistent with all of these predictions.

The trend of A_N for π^0 mesons at lower \sqrt{s} is to increase from zero beginning at a value of x_F which depends on \sqrt{s} [5]. The present results show a similar trend. The significance of the increase of A_N with x_F is 4.7σ (including statistical and point-to-point systematic uncertainties) from a linear fit to the open circles in Fig. 3 for $x_F > 0.27$, with a total $\chi^2 = 0.9$ for 3 degrees of freedom. This is the first significant spin result seen for particles produced with transverse momentum above 1 GeV/c at a polarized proton collider.

In summary, high energy π^0 mesons have been observed from $p_\uparrow + p$ collisions at $\sqrt{s} = 200$ GeV and forward pseudorapidities. The differential cross section is in general consistent with NLO pQCD calculations. The analyzing power is positive and significantly different from zero at large x_F , similar to what was observed in data at $\sqrt{s} \leq 20$ GeV, increasing with x_F above $x_F \approx 0.3$. The analyzing power at $\sqrt{s} = 200$ GeV is in qualitative agreement with pQCD model predictions. Higher precision measurements of A_N as a function of both x_F and p_T may help to differentiate among the models. Future measurements may attempt to determine the Collins fragmentation function in $p_\uparrow + p$ collisions, as well as to look at jet production and Drell-Yan scattering to isolate potential contributions to transverse spin effects.

We thank the RHIC Operations Group and RCF at BNL, and the NERSC Center at LBNL for their support. This work was supported in part by the HENP Divisions of the Office of Science of the U.S. DOE; the U.S. NSF; the BMBF of Germany; IN2P3, RA, RPL, and EMN of France; EPSRC of the United Kingdom; FAPESP of Brazil; the Russian Ministry of Science and Technology; the Ministry of Education and the NNSFC of China; SFOM of the Czech Republic, DAE, DST, and CSIR of the Government of India; the Swiss NSF.

* URL: www.star.bnl.gov

[1] G. L. Kane, J. Pumplin, and W. Repko, Phys. Rev. Lett. **41**, 1689 (1978).
 [2] R. D. Klem *et al.*, Phys. Rev. Lett. **36**, 929 (1976); W. H. Dragoset *et al.*, Phys. Rev. D **18**, 3939 (1978).

[3] S. Saroff *et al.*, Phys. Rev. Lett. **64**, 995 (1990); B. E. Bonner *et al.*, Phys. Rev. D **41**, 13 (1990).
 [4] B. E. Bonner *et al.*, Phys. Rev. Lett. **61**, 1918 (1988); A. Bravar *et al.*, *ibid.* **77**, 2626 (1996); D. L. Adams *et al.*, Phys. Lett. B **261**, 201 (1991); **264**, 462 (1991); Z. Phys. C **56**, 181 (1992).
 [5] K. Krueger *et al.*, Phys. Lett. B **459**, 412 (1999); C. E. Allgower *et al.*, Phys. Rev. D **65**, 092008 (2002).
 [6] A. Airapetian *et al.*, Phys. Rev. Lett. **84**, 4047 (2000); Phys. Lett. B **535**, 85 (2002); **562**, 182 (2003).
 [7] A. Bravar *et al.*, Nucl. Phys. Proc. Suppl. **79**, 520 (1999).
 [8] For a review, see V. Barone, A. Drago, and P. G. Ratcliffe, Phys. Rep. **359**, 1 (2002).
 [9] T. Sjöstrand, Comp. Phys. Commun. **82**, 74 (1994).
 [10] J. Collins, Nucl. Phys. **B396**, 161 (1993).
 [11] D. Sivers, Phys. Rev. D **41**, 83 (1990); **43** 261 (1991).
 [12] M. Anselmino, M. Boglione, and F. Murgia, Phys. Rev. D **60**, 054027 (1999); M. Boglione and E. Leader, Phys. Rev. D **61**, 114001 (2000).
 [13] M. Anselmino, M. Boglione, and F. Murgia, Phys. Lett. B **362**, 164 (1995); M. Anselmino and F. Murgia, *ibid.* **442**, 470 (1998).
 [14] J. Qiu and G. Sterman, Phys. Rev. D **59**, 014004 (1998).
 [15] Y. Koike, AIP Conf. Proc. **675**, 449 (2003); hep-ph/0106260.
 [16] A. Zelenski *et al.*, Proc. of the Part. Acc. Conf. 1999, New York, NY, p. 106.
 [17] G. Bunce *et al.*, Ann. Rev. Nucl. Part. Sci. **50**, 525 (2000); H. Huang *et al.*, Phys. Rev. Lett. **73**, 2982 (1994); M. Bai *et al.*, *ibid.* **80**, 4673 (1998).
 [18] Ya. S. Derbenev *et al.*, Part. Acc. **8**, 115 (1978).
 [19] I. G. Alekseev *et al.*, AIP Conf. Proc. **675**, 812 (2003);
 [20] H. Spinka, AIP Conf. Proc. **675**, 807 (2003).
 [21] O. Jinnouchi *et al.*, AIP Conf. Proc. **675**, 817 (2003).
 [22] J. Tojo *et al.*, Phys. Rev. Lett. **89**, 052302 (2002).
 [23] C. Allgower *et al.*, Nucl. Instr. Meth. **A499**, 740 (2003).
 [24] J. Koryluk, AIP Conf. Proc. **675**, 424 (2003).
 [25] J. Adams *et al.*, nucl-ex/0305015; A. Drees and Z. Xu, Proc. of the Part. Acc. Conf. 2001, Chicago, IL, p. 3120.
 [26] GEANT 3.21, CERN program library.
 [27] F. Aversa *et al.*, Nucl. Phys. **B327**, 105 (1989); B. Jager *et al.*, Phys. Rev. D **67**, 054005 (2003); D. de Florian, *ibid.* **67**, 054004 (2003).
 [28] J. Pumplin *et al.*, J. High Energy Phys. **0207**, 012 (2002).
 [29] P. Aurenche *et al.*, Eur. Phys. J. C **13**, 347 (2000).
 [30] B. A. Kniehl *et al.*, Nucl. Phys. **B597**, 337 (2001).
 [31] S. Kretzer, Phys. Rev. D **62**, 054001 (2000).
 [32] S. S. Adler *et al.*, hep-ex/0304038.